Published in final edited form as:
Cancer Cell. 2012 September 11; 22(3): 291–303. doi:10.1016/j.ccr.2012.07.023.

TGF-β-miR-34a-CCL22 Signaling-Induced Treg Cell Recruitment Promotes Venous Metastases of HBV-Positive Hepatocellular Carcinoma

Pengyuan Yang[1,5], **Qi-Jing Li**[2], **Yuxiong Feng**[3], **Yun Zhang**[1], **Geoffrey J. Markowitz**[1], **Shanglei Ning**[1], **Yuezhen Deng**[3], **Jiangsha Zhao**[3], **Shan Jiang**[2], **Yunfei Yuan**[6], **Hong-Yang Wang**[4], **Shu-Qun Cheng**[4], **Dong Xie**[3,*], and **Xiao-Fan Wang**[1,*]

[1]Department of Pharmacology and Cancer Biology, Duke University Medical Center, Durham, NC 27710, USA

[2]Department of Immunology, Duke University Medical Center, Durham, NC 27710, USA

[3]Laboratory of Molecular Oncology, Institute for Nutritional Sciences, Shanghai Institutes of Biological Sciences, Shanghai 200031, China

[4]The Eastern Hepatobiliary Surgery Hospital, Second Military Medical University, Shanghai 200433, China

[5]Department of Pharmacology & School of Pharmacy, Second Military Medical University, Shanghai 200433, China

[6]Department of Hepatobiliary Surgery, Sun Yat-sen University Cancer Center, Guangzhou 510060, China

Abstract

Portal vein tumor thrombus (PVTT) is strongly correlated to a poor prognosis for patients with hepatocellular carcinoma (HCC). In this study, we uncovered a causative link between hepatitis B virus (HBV) infection and development of PVTT. Mechanistically, elevated TGF-β activity, associated with the persistent presence of HBV in the liver tissue, suppresses the expression of microRNA-34a, leading to enhanced production of chemokine CCL22, which recruits regulatory T (Treg) cells to facilitate immune escape. These findings strongly suggest that HBV infection and activity of the TGF-β-miR-34a-CCL22 axis serve as potent etiological factors to predispose HCC patients for the development of PVTT, possibly through the creation of an immune-subversive microenvironment to favor colonization of disseminated HCC cells in the portal venous system.

*Correspondence to: Xiao-Fan Wang, Department of Pharmacology & Cancer Biology, Duke University Medical Center, Duke University, Box 3813, Research Drive, Durham, NC 27710, USA. Tel.: +1-919-681-4861; Fax: +1-919-681-7152; wang0011@mc.duke.edu or Dong Xie, Laboratory of Molecular Oncology, Institute for Nutritional Sciences, Shanghai Institutes for Biological Sciences, Chinese Academy of Sciences and Graduate School of Chinese Academy of Sciences, Shanghai20031, China. Fax: (86)-21-54920291; dxie@sibs.ac.cn.

INTRODUCTION

Hepatocellular carcinoma (HCC) is one of the major health problems worldwide (Parkin et al., 2005). Since HCC is often diagnosed at an advanced stage, a large proportion of HCC patients display symptoms of intrahepatic metastases or postsurgical recurrence (Portolani et al., 2006), with a five-year survival rate of around only 30%–40%. In about a third of those instances, metastatic tumors colonize the major branches of the portal vein with the clinical symptom termed portal vein tumor thrombus (PVTT) (Chambers et al., 2002), although the mechanism underlying the formation of PVTT remains largely unknown. Interestingly, almost all the reported PVTT cases in the literature have been from developing countries, suggesting that this particular pathological symptom may not be common in HCC patients in developed countries.

The development of HCC is believed to be associated with hepatitis B virus (HBV) and hepatitis C virus (HCV) infection, carcinogen/toxin exposure and/or genetic factors. Among these suspected etiological factors, HBV infection accounts for more than 60% of the total liver cancer in developing countries and less than a quarter of cases in developed countries (Jemal et al., 2011). The HBV-initiated tumorigenic process often follows from or accompanies long-term symptoms of chronic hepatitis, inflammation and cirrhosis. The HBV infection-triggered inflammatory and/or fibrotic process, with extensive involvement of cytokine/chemokine production/activation and leukocytes infiltration, is believed to create a microenvironment that favors the development of HCC. Consistent with an important role for HBV in HCC, persistent presence of HBV DNA in the serum of infected individuals is found to be a strong indicator for the development of HCC (Chen et al., 2006). Moreover, HCC patients with high levels of serum HBV DNA have a poor prognosis, including risks of death, metastasis and recurrence following surgery (Chen et al., 2009). However, it remains unclear whether the HBV-initiated pathological process plays a specific role in late stages of HCC progression, such as formation of PVTT.

The cytokine TGF-β is known to be a multi-functional factor that plays critical roles in various aspects of liver pathogenesis, including chronic HBV/HCV infection (Marotta et al., 2004), cirrhosis (Matsuzaki, 2009), and tumorigenesis (Massague, 2008). Mounting evidence indicates that one efficacious mechanism by which TGF-β promotes tumor progression and metastasis is through repression of immune-surveillance within the tumor microenvironment (Bierie and Moses, 2006; Massague, 2008; Schmierer and Hill, 2007): TGF-β can attract several types of innate and adaptive immune cells to the tumor sites, enhance production of various cytokines/chemokines, and alter the functional differentiation program of those cells, consequently promoting tumor growth, invasion, and metastasis (Massague, 2008).

Within the tumor microenvironment, FoxP3-expressing regulatory T (Treg) cells, which normally function as a dominant inhibitory component in the immune system to actively maintain self-tolerance and immune homeostasis through suppression of various immune responses, have been demonstrated to be coopted by tumor cells to escape immune-surveillance (Mailloux and Young, 2010). Treg cells are frequently found to accumulate within the tumor mass and ascites (Quezada et al., 2006). A number of chemokines including CCL22 that is also termed macrophage-derived chemokine (MDC) and originally found to be secreted by macrophages and dendritic cells upon stimulation with microbial products, have been shown to recruit Treg cells to modulate the immune response during the tumorigenic process (Curiel et al., 2004). Although TGF-β has been found to regulate the development of natural Treg cells in the thymus during negative selection (Ouyang et al., 2010) and the extra-thymical conversion of conventional T cells into suppressive inducible

Treg cells (Chen et al., 2003), it is unclear whether TGF-β contributes to the accumulation of natural Treg cells within the tumor microenvironment.

MicroRNAs (miRNAs) are small non-coding RNAs of ~22 nucleotides that negatively regulate gene expression by blocking protein translation and promoting degradation of the target messenger RNA (Bartel, 2004). Changes in the expression profiles of miRNAs have been linked to the development of various types of human diseases, including cancer (Lujambio and Lowe, 2012). MicroRNAs can act as oncogenic promoters or tumor suppressors, depending on the functional nature of their specific target genes within a specific cell or tissue type (Esquela-Kerscher and Slack, 2006; Nicoloso et al., 2009). In the context of HCC, recent reports indicate that alterations in the expression levels of specific miRNAs are closely associated with specific stages of the disease process, including intrahepatic metastasis (Ding et al., 2010; Xiong et al., 2010). However, those studies did not elucidate the specific roles of any those microRNAs in the progression of HCC to venous metastasis. In this study, we explored the possibility that specific miRNAs could act as mediators of changes in the tumor microenvironment during HCC progression and whether there was a potential link between HBV status as an etiological factor and development of HCC-PVTT.

RESULTS

HBV infection status and TGF-β signaling activity are positively associated with PVTT development in HCC patients

To investigate whether there is an etiological basis for the development of PVTT, we analyzed the clinical data of 288 HCC patients who received treatment in the Shanghai Eastern Hepatobiliary Surgery Hospital and Guangzhou Sun Yat-sen University Cancer Center in China (Table 1). Among those patients, 234 developed PVTT with a poor prognosis in comparison to the 54 patients who were negative for symptoms associated with PVTT (Figure 1A). Within the PVTT positive group, the prognosis of the patients showed a clear correlation with the types of PVTT development (Shi et al., 2010) as measured by the presence of tumor lesions in different segments of the portal venous system (Figure 1B).

In contrast to developed countries, HBV infection is the major causative factor of HCC in China and other developing countries with HBV^+ status accounting for as much as 80% of all HCC cases. In our patient cohort, 89% of the 234 HCC patients with PVTT who were examined for their HBV status were HBV^+ but only 68% of 60 HCC patients without PVTT are HBV^+ (Figure 1C). This indicates that HBV infection status is strongly associated with the development of PVTT, which was not noted previously likely because PVTT has not been reported as a major pathological feature of HCC patients in developed countries. Consistent with a poorer prognosis of HCC patients who develop PVTT, HBV^+ patients showed a much worse prognosis than HBV^- patients (Figure 1D). Taken together, the clinical data on our patients strongly support the notion that HBV infection is a potent etiological factor predisposing HCC patients to develop PVTT with a poor prognosis of the disease.

To investigate possible mechanisms underlying the observed link between positive HBV status and the development of PVTT, we conducted further analysis on the pathological characteristics of the 234 PVTT patients whose clinical history was recorded in more detail. It has been well established that chronic HBV infection is associated with induction of inflammation, fibrosis, or even cirrhosis prior to the development of HCC. Indeed, 219 patients were recorded to have liver cirrhosis or their tumor were found to display pathological features of inflammation and fibrosis at the time of surgery (Figure 1E). Since TGF-β is among the most potent cytokines linked to liver inflammation, fibrosis and

cirrhosis (Bissell, 2001), we next determined the level of TGF-β signaling activity by measuring the status of Smad2 phosphorylation in the nucleus using tissue microarrays prepared from some of the 294 HCC patient samples. Strong nuclear p-Smad2 staining, with a score of IHC intensity over 2 (++), was detected in 11 of 16 PVTT tumor specimens and 22 of 66 HBV^+ primary HCC tumor samples. In contrast, 7 of 10 HBV^- HCC tumor samples showed very low p-Smad2 levels with a score of IHC intensity less than 1 (+) (Figure 1F). Consistent with the IHC results, the levels of p-Smad2 determined by Western blot from fresh tumor tissues were also found to be significantly higher in HBV^+ HCC primary and PVTT tissue samples compared with those of HBV^- tumors (Figure S1). These data indicate that high levels of TGF-β signaling activity are strongly associated with the development of HBV^+ primary HCC and PVTT.

We also measured the expression of TGF-β1, the main isoform of the TGF-β family, in several liver cell lines, including WRL68 (non-tumorigenic and HBV^-), HepG2 (HBV^- liver tumor cells), HepG2.2.15 (HepG2-derivative with integration of the HBV genome) (Delaney and Isom, 1998), and PVTT-1 (established from a PVTT biopsy sample of a HBV^+ HCC patient). As shown in Figure 1G, TGF-β1 expression is much higher in HBV^+ than in HBV^- cell lines, providing support to the notion that TGF-β may play a role in the progression of HBV-initiated HCC to PVTT. To test whether HBV could have a more direct effect on the expression of TGF-β, we transiently transfected HepG2 cells with two HBV-encoded genes HBx and HBs that have been reported to play functional roles in HBV-associated carcinogenesis (Lupberger and Hildt, 2007). Interestingly, transient expression of these genes leads to increased TGF-β1 levels in the cell supernatants within 24 hrs in a dose-dependent manner (Figure 1H). These results suggest that the presence of HBV encoded genes could have a direct influence on TGF-β expression in liver cancer cells.

Expression of miR-34a is inversely correlated with metastatic potential in HBV^+ HCC and subject to negative regulation by TGF-β

We then screened WRL68, HepG2, PVTT-1, and MHCC97 cell lines using a qRT-PCR-based microRNA-array strategy to identify microRNAs that may be functionally linked to HCC metastases. MHCC97 is a HBV^+ cell line that acquired metastatic capacity through passages in nude mice (Tian et al., 1999). As shown in Figure 2A and Table S1, the expression of a group of microRNAs displays significant differences among these four cell lines. The miR-34a, but not its family members miR-34b/c, level is significantly lower in both HBV^+ PVTT-1 and MHCC97 lines with high metastatic potential than in the other two cell lines (Figure 2B). We selected miR34a for further investigation because it is a well-established tumor suppressor (He et al., 2007) and it was one of the 20-miRNA signature for prediction of developing HCC venous metastasis and poor prognosis when its expression is reduced in primary HCC tumors at the time of diagnosis (Budhu et al., 2008).

We next determined whether this suppressed miR-34a expression represents a general pattern in HCC patients with different HBV and PVTT status. We selected clinical samples from the original 294 patients shown in Figure 1C based on the initial evaluation of quality of RNA extracted from the tissue specimen, and analyzed the expression of miR-34a using qPCR from 26 PVTT tissue samples (all were HBV^+), 30 primary tumor tissue samples (17 HBV^+ and 13 HBV^-), and 14 normal liver tissues derived from areas distal to tumor lesions. As shown in Figure 2C, the level of miR-34a was significantly lower in a large fraction of the HBV^+ primary and PVTT tumor samples than that of the HBV^- primary tumor or normal liver tissues. Together these data suggest that reduction in miR-34a expression is frequently associated with HBV-initiated HCC during the disease progression towards the development of PVTT.

To determine whether TGF-β could have a direct role in regulating miR-34a expression, we treated three HCC cell lines with TGF-β and measured the levels of miR-34a at various time points. TGF-β induced a rapid and robust reduction of mature miR-34a in all of these cell lines, even though the basal level of this miRNA in PVTT-1 cells was already very low (Figure 2D). Interestingly, the basal level of miR-34a in the HBV^+ HepG2.2.15 cells was also reduced in comparison to their parental HepG2 cells, indicating that presence of the HBV genome could lead to suppression of miR-34a expression (Figure 2D), possibly through the autocrine action of TGF-β1 produced by the same cells (Figure 1G). To test this possibility, we treated HepG2.2.15 cells with SB431542, an inhibitor of the type I TGF-β receptor kinase, and found an increase in the level of miR-34a after blocking autocrine TGF-β signaling activity (Figure S2). Taken together with data shown in Figure 1, these results indicate that reduction in miR-34a expression in HBV^+ HCC primary and PVTT tumor samples could be directly linked to the high level of TGF-β signaling activity.

The primary target of miR-34a in PVTT cells is the chemokine gene *CCL22*

We initially speculated that previously reported targeting CDK4, CCNE2 and MET by the miR-34a/b/c family (He et al., 2007) could be the potential mechanism underlying the association between the reduced miR-34a expression and HCC-PVTT development. However, we did not observe an inhibitory effect on cell viability and proliferation, or any difference in cell migration when miR-34a mimic oligos were transfected into PVTT-1 cells (Figures S3A–S3C). Moreover, there were only slight negative effects observed on mRNA levels of these three reported target genes with the presence of high level miR-34a in those cells (Figure S3D). Ectopic expression of miR-34a also did not affect the growth of PVTT-1 tumors in vivo (Figures S3E–S3G). These negative results strongly suggest that, should miR-34a have a tumor-suppressive effect on the development of HCC-PVTT, it likely acts through a cell non-autonomous mechanism.

One possible cell non-autonomous route for miR-34a to execute its tumor-suppressive function is to impact the tumor microenvironment by regulating the production of secreted proteins. To test this hypothesis, we developed a qPCR-based assay (Figure S3H) to investigate the potential effect of this miRNA on the expression of cytokines, chemokines, and their receptors in PVTT-1 cells and identified the chemokine CCL22 as the most significantly down-regulated molecule upon miR-34a overexpression (Figure 3A). In parallel, we employed established bioinformatic procedures to predict putative miR-34a target genes and identified CCL22 among the top hits associated with tumor metastasis. There are three putative miR-34a targeting sequences present in the 3'-UTR of the human *CCL22* (Figure 3B), two of which were also found in the murine *Ccl22* (data not shown). To determine if miR-34a affect the expression of CCL22 through these putative targeting elements, we employed a luciferase reporter carrying these elements. A control construct was also generated in which the three putative miR-34a targeting sequences were mutated. As shown in Figure 3C, expression of the miR-34a-mimic oligos significantly suppressed the luciferase activity of the wild type reporter in a dose-dependent manner but had minimal effect on the mutant reporter, supporting the notion that CCL22 is a *bona fide* target of miR-34a.

To further validate CCL22 as a legitimate target of miR-34a, we examined the expression of the endogenous CCL22 when miR-34a expression was manipulated. As shown in Figure 3D, ectopic expression of miR-34a significantly reduced CCL22 mRNA level. Interestingly, overexpression of miR-34b/c was much less potent in reducing the expression of CCL22 (Figure S3I), even though they share the same seed targeting sequence as miR-34a. Corresponding to a reduction in the level of CCL22 mRNA, the secretion of CCL22 protein was also drastically diminished with miR-34a ectopic expression (Figure 3E). Reciprocally, introduction of antisense (AS)-miR34a oligos into the PVTT-1 cells was accompanied by an

increase in CCL22 production in a dose-dependent manner (Figure 3F). To examine this further, we also transfected the AS-miR34a oligos into HepG2 cells which have a relatively higher basal level of miR-34a compared to that of PVTT-1 cells (Figure 2B), and detected an increase in the level of CCL22 mRNA (Figure S3J). Taken together, these data suggest that the expression of miR-34a and CCL22 is inversely correlated, most likely through the direct targeting of the CCL22 gene by miR-34a.

An inverse relationship between the CCL22 level and the miR-34a level is observed in HBV$^+$ HCC tumor samples

We next determined the expression pattern of CCL22 in four cell lines with different HBV status. As shown in Figure 4A, higher protein levels of CCL22 were detected in HBV$^+$ (miR-34a low) HepG2.2.15 and PVTT-1 cells than in HBV$^-$ (miR-34a high) WRL68 and HepG2 cells. We then measured mRNA levels of CCL22 by qPCR using the same set of tissue samples shown in Figure 2C and found that CCL22 mRNA level was significantly increased in the group of HBV$^+$ primary tumors and further elevated in PVTT samples (Figure 4B). Importantly, the CCL22 mRNA level is inversely associated with the miR-34a level in HBV$^+$ primary tumor and PVTT tumors when the values for each individual patient were plotted (Figure 4C). In contrast, such association is not observed in HBV$^-$ tumor samples or normal liver tissues (Figure 4C). Again, these clinical data provide strong support for our hypothesis that the elevation in CCL22 is likely the result of reduced expression of miR-34a with a close association with the positive status of HBV as the etiological factor in the development of PVTT.

Reduced miR-34a expression is correlated with enhanced recruitment of T regulatory cells

CCL22 has been implicated in the tumorigenic process by binding to its receptor CCR4 on the surface of Treg cells, consequently recruiting those immunosuppressive cells to the tumor microenvironment and promoting tumor cell escape from immune-surveillance. Thus, miR-34a may exert its cell non-autonomous tumor-suppressive effect by regulating CCL22 expression and recruitment of Treg cells. To test this hypothesis, we examined the ability of culture media from PVTT-1 cells treated with different concentrations of AS-miR-34a oligos to mobilize CD4$^+$CD25$^+$ cells freshly isolated from healthy donors, the majority of which were FoxP3$^+$ Treg cells (Figure S4A). As shown in Figure 5A, inhibition of miR-34a correlates with increase in the migratory activity of the Treg cells. Furthermore, anti-human CCL22 neutralizing antibody significantly inhibited the enhanced Treg cell migratory activity, indicating that miR-34a inhibitor-induced Treg cell migration is dependent on the production of CCL22.

To investigate the role of miR-34a in regulating Treg cell migration *in vivo*, we inoculated PVTT-1 cells with or without ectopic expression of miR-34a into nude mice to form tumors and transferred freshly isolated CD4$^+$CD25$^+$ human Treg cells into those mice via tail vein injection 14 days later. Together with determination of the expression status of CCL22 (Figure 5B), the accumulation of human Treg cells inside the PVTT tumors was assessed 48 hrs later. As shown in Figures 5C and S4B, miR-34a ectopic expression in PVTT-1 cells significantly decreased accumulation of CD4$^+$CD25$^+$ Treg cells but not CD4$^+$CD25$^-$ T cells inside the tumor.

To investigate whether there is a link between the expression of miR34a and the level of Treg cells present in clinical samples, we determined the expression profile of FoxP3, which is expressed primarily if not exclusively in Treg cells, in the same set of tissue specimen used in experiments presented in Figures 2C and 4B. We observed higher levels of FoxP3 mRNA in HBV$^+$ primary and PVTT tumor tissues (Figure 5D), indicating a greater accumulation of Treg cells in HBV$^+$ primary and PVTT tumor tissues. Indeed, this

postulation is supported by immunohistochemical staining of a subset of the tumor specimens (Figure 5E). Again, analyzed at the individual patient level, the increase of FoxP3 mRNA inside the tumor mass is strongly associated with the decrease of miR-34a level in HBV^+ primary and PVTT tumors (Figure 5F). Together these results provide strong support to the notion that the suppression of miR-34a in HBV^+ primary and PVTT tumor cells leads to elevated production of CCL22 in the tumor microenvironment, which in turn augments the recruitment of Treg cells and immune suppression.

TGF-β induces CCL22 production via suppression of miR-34a

We then tested whether TGF-β could affect CCL22 expression. As shown in Figure 6A, CCL22 production by PVTT-1 cells was increased following TGF-β treatment in a time-dependent manner. To determine whether TGF-β exerts its effect via the canonical signaling pathway, we added SB431542 to the PVTT-1 cells in the presence or absence of TGF-β. SB431542 completely blocked the ability of TGF-β to suppress miR-34a or to induce CCL22 expression (Figure 6B). We also observed that forced miR-34a elevation dose-dependently blocked the ability of TGF-β to induce the expression of CCL22 in PVTT-1 cells (Figure 6C), suggesting that the effect of TGF-β on CCL22 expression was predominantly mediated by down-regulation of miR-34a. The functional relationship between miR-34a and TGF-β observed here is similar to the previous reported inhibition of TGF-β-induced epithelial-mesenchymal transition by ectopic miR-34a expression (Siemens et al., 2011).

We next investigated the role of this TGF-β-miR-34a-CCL22 pathway on Treg cell migration. Culture media from PVTT-1 cells treated with different concentrations of miR-34a mimic oligos were tested for their capacity to mobilize freshly isolated human $CD4^+CD25^+$ Treg cells. Consistent with the enhanced CCL22 production, Treg cell migratory activity was correspondingly increased upon exposure to supernatant derived from PVTT-1 cells treated with TGF-β (Figure 6D). On the other hand, transfection of miR-34a mimic oligos into the PVTT-1 cells blocked the effect of TGF-β-induced CCL22 expression and Treg cell migration in a dose-dependent manner (Figure 6D).

The suppressive function of miR-34a on tumor growth and metastasis is mediated by CCL22

The miR-34a-CCL22-Treg link demonstrated above provides us with a plausible explanation for why miR-34a has little impact on xenograft tumor formation by human PVTT-1 cells in athymic nude mice (Figures S3F, S3G): the hosts have no T cells (including Tregs) and exhibit little cellular immunity. The use of murine model systems in which liver tumorigenesis can be induced by gene manipulation or chemicals has very limited application or relevance for our purpose since HBV is not an etiological factor for the initiation of liver tumor formation in those established models. Nevertheless, we have adopted a model by employing a murine liver tumor cell line, Hepa1-6, originally derived from the C57BL/6J mouse strain that is immune-competent with fully functional T cell lineages. Consistent with what shown in Figures S3F and S3G, we found that miR-34a overexpression has minimal effect on Hepa1-6 tumor growth in nude mice (Figure 7A), even though tumors derived from Hepa1-6 cells express a low level of CCL22 that was reduced by the ectopic expression of miR-34a (Figure 7B). In order to test the full potential of CCL22 to promote tumor metastasis in the context of an immune-competent host, we engineered ectopic expression in Hepa1-6 cells of the mouse CCL22 open reading frame (ORF) without its 3'-UTR so that it cannot be targeted by miR-34a. Indeed, overexpression of CCL22 was not affected by the co-expression of miR-34a (Figure 7B). Subsequently, these four populations of Hepa1-6 cells were inoculated subcutaneously into C57BL/6J mice, and tumor growth was followed for 21 days. As shown in Figure 7C, Hepa1-6 tumor

growth was significantly suppressed by miR-34a overexpression in immune-competent mice in comparison to that of the vector control. In contrast, CCL22 overproduction appeared to have a dramatic positive effect on tumor growth. Importantly, miR-34a-induced tumor suppression was largely eliminated upon the overexpression of the non-targetable CCL22 (Figure 7C), strongly suggesting that the tumor-suppressive effect of miR-34a was mediated by reducing the production of CCL22 as its predominant target. To further investigate the mechanism by which miR-34a and CCL22 exert their effects on the growth of Hepa1-6 cells in their syngeneic and immune-competent hosts, we quantified the number of Treg cells infiltrated into the tumor mass formed by the four types of cells. Consistent with the role of CCL22 as a chemo-attractant predominantly for Treg cells, the number of $CD4^+CD25^+FoxP3^+$ cells detected in tumors correlated with the level of CCL22 produced by each population of Hepa1-6 cells (Figure 7D).

Using the same set of four populations of Hepa1-6 cells, we assessed the effects of miR-34a and CCL22 on metastatic potential following a well-established protocol (Bao et al., 2004; Feng et al., 2011). The different batch of Hepa1-6 cells carrying a luciferase reporter was inoculated intrasplenically into C57BL/6J mice. After 21 days, luciferase signals derived from abdominal metastatic growth were measured by the Xenogen IVIS Lumina system. As shown in Figures 7E–7G, ectopic miR-34a expression significantly reduced metastatic growth. In contrast, CCL22 had a potent effect in boosting the growth of Hepa1-6 cells inside the mouse liver and abdomen, completely overcoming any inhibitory effect by miR-34a (Figures 7E–7G).

To provide further support for the role of miR-34a in promoting tumor metastasis using a different immune-competent mouse model and to assess whether this miR-34a-CCL22-Treg pathway can function in a different tumor context, we employed a well-established mouse model of lung metastasis by 4T1 murine mammary tumor cells in their syngeneic hosts of the BALB/c background (Morecki et al., 1998). We first determined that miR-34a overexpression has the same negative effect on CCL22 production in 4T1 cells as in human PVTT-1 cells (Figure S5A). We then inoculated 2×10^4 4T1 cells with or without miR-34a overexpression into the mammary fat pad of female BALB/c mice. Consistent with the results shown in Figure 7C, the size of tumors from 4T1 cells ectopically expressing miR-34a was smaller than that of control cells after 21 days of growth (Figure S5B). To test if Treg cells were differentially recruited to the 4T1 tumors upon manipulation of tumor miR-34a levels, we quantified the number of $CD4^+CD25^+FoxP3^+$ Treg cells inside the tumor mass of the collected primary tumor tissue. A significant reduction in the number of Treg cells was observed from tumors derived from 4T1 cells with ectopic miR-34a expression (Figure S5B). To gain further insight using this system, we repeated these experiments by implanting 5×10^4 4T1 cells. Seven or fourteen days post-implantation, mice were subjected to imaging analysis to quantify the metastatic tumor mass in the lung. As shown in Figure S5C, ectopic miR-34a expression completely blocked the formation of lung metastases by the 4T1 cells, likely through the reduction of CCL22. Taken together, our results from both liver and mammary tumor models demonstrate the potent anti-metastatic effect of miR-34a, which is mediated primarily by suppressing Treg cell recruitment via inhibition of CCL22 production.

DISCUSSION

The presence of PVTT in patients with HCC is one of the most significant factors for a poor prognosis in developing countries (Lin et al., 2010; Shi et al., 2010). Once PVTT is formed, the tumor cells may spread along the portal vein, leading to extensive bilobar intrahepatic metastasis. Portal vein obstruction also causes further deterioration in liver function, often resulting in liver failure. In addition, PVTT-induced portal hypertension can cause

intractable ascites and esophageal variceal bleeding. The symptoms associated with PVTT present a major challenge for the treatment of HCC in such patients. Despite its clinical importance, however, the mechanism associated with the pathogenesis of PVTT remains largely unclear.

In the current study, we extensively investigated the risk factors and mechanism underlying the development of this important intrahepatic metastasis. Consistent with a previous report (Takizawa et al., 2007), PVTT also strongly correlates with poor prognosis in our cohort of HCC patients. Importantly, we uncovered a link between the development of PVTT and positive HBV infection status, as well as high level of TGF-β signaling activity. Compared with a rate of 14.3% of PVTT metastasis in HBV^- HCC patients, a much higher rate of 82.5% of PVTT development was found among HBV^+ patients. Thus, our findings strongly suggest that HCC initiated by HBV infection predisposes those patients for development of PVTT, which in turn accounts for the high mortality rate for HCC patients in the developing countries, such as China (Jemal et al., 2011), where a large population has been exposed to HBV infection and become chronic carriers of the virus (Han, 2009).

Consequently, HCC should be stratified to at least two major categories based on the pathological nature of the likely initiating step of tumorigenesis associated with the dominant etiological factor: HBV (possibly HCV as well) infection verses other causes, such as toxin exposure or alcoholism-induced cirrhosis. One protein encoded by the HBV genome, HBx, has been well established to play a critical role in HBV-associated liver pathogenesis, including tumorigenesis by functioning as an oncogene (Benhenda et al., 2009; Kew, 2011). Together with inactivation of p53 and activation of the Wnt pathway commonly detected in HCC (Ding et al., 2005; Feitelson and Duan, 1997), HBx and possibly other HBV-encoded proteins could act as the drivers for HCC initiation and progression. In the meantime, pathological changes associated with the HBV-initiated tumorigenic process, both cell autonomous and non-autonomous, that predispose patients to the development of PVTT, could be distinct from those genetic and epigenetic alterations in hepatocytes and their microenvironment induced by etiological factors other than HBV (Herceg and Paliwal, 2011). In this regard, treatment options should be developed that tailor to the specific molecular nature of HCC pathogenesis associated with HBV to improve the prognosis of those patients.

The full spectrum of pathological factors that contribute to the development of PVTT of HBV^+ HCC patients remain to be adequately elucidated, mainly because the lack of a suitable mouse model system that could faithfully and more completely mimic the pathological process of tumor thrombosis formation in human HCC patients since HBV is incapable of infecting mouse hepatocytes. Nevertheless, our discovery of the TGF-β-miR-34a-CCL22 pathway, which could render the microenvironment of liver tissue around the portal venous system immunosuppressive to favor the colonization and expansion of HCC cells disseminated from the primary tumor site, represents a major step towards addressing this critical question. Following HBV infection and during subsequent pathological processes, such as inflammation and/or fibrosis, a change in the liver microenvironment may begin with a significant increase in the activity of TGF-β signaling, which in turn suppresses the expression of miR-34a, resulting in the enhanced production of the chemokine CCL22 and recruitment of Treg cells. The potent immune-suppressive activity of Treg cells causes subversion of immune responses against tumor cells escaped from the primary tumor, leading to the development of intrahepatic venous metastasis. In this regard, CCL22, a secreted molecule capable of acting on both tumor and immune cells, could be considered as a potential therapeutic target for the development of an effective treatment for this disease.

The paradoxical results from the different phenotypes of miR-34a-overexpressing tumor cells in immune-compromised nude mice and in immune-competent C57BL/6J and BALB/c mice provided the key evidence that this miR-34a-CCL22 pathway plays a central role in modulating the tumor immune microenvironment. A wealth of evidence suggests that Treg cells, especially $CD4^+CD25^+$ Treg cells, act to sustain self-tolerance and immune homeostasis by suppressing a wide variety of physiological and pathological immune responses against self and non-self, as well as quasi-self tumor antigens (Sakaguchi, 2004; Shevach, 2002). However, how these naturally arising Treg cells are recruited into the tumor microenvironment to negatively control immune tumor surveillance has remained largely unknown. Several studies indicated that TGF-β could induce naïve T cell differentiation into Treg cells (Liu et al., 2008), consistent with the close association in expression profiles of TGF-β and Treg cell marker FoxP3 in multiple types of human tumors. However, this function for TGF-β signaling in regulating the development of natural Treg cells cannot adequately explain the observed recruitment of Treg cells into tumor microenvironment, which is particularly important for tumor progression and metastasis. In this regard, our findings provide the critical experimental evidence on the important roles of TGF-β and cytokines/chemokines induced by TGF-β in the creation of a favorable microenvironment for tumor metastasis through regulation of Treg cell recruitment.

EXPERIMENTAL PROCEDURES

Patients and Tissue Samples

Clinical samples were obtained from 288 HCC patients treated at the Shanghai Eastern Hepatobiliary Surgery Hospital and Guangzhou Sun Yat-sen University Cancer Center in China. Among those patients, 234 were diagnosed with developed PVTT and the 54 patients were negative for symptoms associated with PVTT. Within the PVTT positive group, the types of PVTT development as measured by the presence of tumor lesions in different segments of the portal venous system (Shi et al., 2010). All the samples and associated clinical information were collected with informed consent of patients and all the experiments were approved by the Internal Review and Ethics Boards of the Shanghai Eastern Hepatobiliary Surgery Hospital and Guangzhou Sun Yat-sen University Cancer Center, respectively.

Cell Culture

HepG2, Hepa1-6 and WRL68 cells were obtained from ATCC and cultured under standard conditions. PVTT-1 cells have been described previously (Wang et al., 2010). MHCC97 cells were obtained from Dr. Z. Tang. 4T1 cells were obtained from Dr. R.A. Weinberg. $CD4^+CD25^+$ T cells and $CD4^+CD25^-$ T cells were separately purified with Dynabeads Regulatory $CD4^+CD25^+$ T cell kits (Invitrogen) from human blood (purchased from Gulf Coast Regional Blood Center, Houston, TX).

Reagents and plasmids

AS-miR-34a and scramble control LNA oligonucleotides were purchased from Exiqon (Vedbaek, Denmark). Pre-miR-34a mimic processor and scramble control oligonucleotides were purchased from Ambion. The miR-34a and miR-34b/c expression vectors were constructed using TRIPZ lentiviral system from Thermo Scientific Open Biosystems.

miRNA Detection

Total RNA, inclusive of the small RNA fraction, was extracted from cultured cells with a mirVana miRNA Isolation Kit (Ambion). RT-PCR-based array for detection of mature miRs and U6 was achieved with gene-specific primers.

Animal Studies

All research involving animals complied with protocols approved by the Duke University Animal Care and Use Committee. The in vivo migration assays were measured following an established method (Curiel et al., 2004). For spontaneous metastasis assays, the metastatic formation was monitored by the appearance of luciferase activities by imaging apparatus of IVIS systems.

MTT and BrdU assays

In vitro cell viability was measured by MTT assay following established protocols (Feng et al., 2011). A BrdU incorporation assay was conducted according to the manufacture's instruction (BD Pharmingen, San Diego, CA).

Immunoblots

Cell lysates and supernatants were resolved by electrophoresis, transferred to a PVDF membrane, and probed with antibodies against γ-tubulin (Santa Cruz) or CCL22 (R&D Systems).

Immunohistochemistry

Detection of phospho-Smad2 (Cell Signaling Technology) and FoxP3 (Abcam) was performed on 5 μm paraffin sections of tissue samples with the indicated antibodies, using Vectastain Elite ABC kits (Vector), and ImmPACT DAB Substrate (Vector). For pSmad2, the score was evaluated as 4 levels from 0 (−), 1(+), to 2(++), 3(+++).

FACS

Cells were stained with monoclonal antibodies and analyzed on a FACSCanto (Becton-Dickinson). Antibodies were mouse anti-human CD4-APC (Biolegend), mouse anti-human CD25-PE (Biolegend), mouse anti-human FoxP3-PB (Biolegend), PB anti-mouse CD4 (eBioscience), PE anti-mouse CD25 (eBioscience), and PE-Cy5 anti-mouse/rat Foxp3 (eBioscience).

Migration Assay

Cell migration was assessed as described (Curiel et al., 2004) using $CD4^+CD25^+$ Treg cells. PVTT-1 tumor cell supernatants were added to the lower chamber. Antibody against CCL22 and control IgG were obtained from R&D Systems.

Statistical Analyses

Data are presented as mean ± S.D. Student's t test was used for comparisons.

Supplementary Material

Refer to Web version on PubMed Central for supplementary material.

Acknowledgments

We wish to thank J. Lee and I. Liu for help with the use of 4T1/BALB/c mouse model, L. Su and J. Gao for Treg cell purification and IHC for Foxp3, X. Cao for advice on tumor immunology, L. He for providing the miR-34b/c plasmid, Y. Gao in Duke University Light Microscopy Core Facility for imaging experiments, the CCIF and Cell Sorting Facility of Duke Cancer Institute for animal care and cell sorting experiments, respectively. Q.-J. L. is a Whitehead Family Foundation Scholar and the research reported in this publication was supported by the Research Scholar Grant RSG-10-157-01-LIB from the American Cancer Society to Q.-J. L., Ministry of Science and Technology Key Program of China 2012ZX10002009-017 and National Basic Research Program of China

2010CB912102 to D. X., and the National Cancer Institute of the National Institutes of Health under award number CA151541 to X.-F. W.

REFERENCES

Bao S, Ouyang G, Bai X, Huang Z, Ma C, Liu M, Shao R, Anderson RM, Rich JN, Wang XF. Periostin potently promotes metastatic growth of colon cancer by augmenting cell survival via the Akt/PKB pathway. Cancer Cell. 2004; 5:329–339. [PubMed: 15093540]

Bartel DP. MicroRNAs: genomics, biogenesis, mechanism, and function. Cell. 2004; 116:281–297. [PubMed: 14744438]

Benhenda S, Cougot D, Buendia MA, Neuveut C. Hepatitis B virus X protein molecular functions and its role in virus life cycle and pathogenesis. Advances in cancer research. 2009; 103:75–109. [PubMed: 19854353]

Bierie B, Moses HL. Tumour microenvironment: TGFbeta: the molecular Jekyll and Hyde of cancer. Nat Rev Cancer. 2006; 6:506–520. [PubMed: 16794634]

Bissell DM. Chronic liver injury, TGF-beta, and cancer. Exp Mol Med. 2001; 33:179–190. [PubMed: 11795478]

Budhu A, Jia HL, Forgues M, Liu CG, Goldstein D, Lam A, Zanetti KA, Ye QH, Qin LX, Croce CM, et al. Identification of metastasis-related microRNAs in hepatocellular carcinoma. Hepatology. 2008; 47:897–907. [PubMed: 18176954]

Chambers AF, Groom AC, MacDonald IC. Dissemination and growth of cancer cells in metastatic sites. Nat Rev Cancer. 2002; 2:563–572. [PubMed: 12154349]

Chen CJ, Yang HI, Iloeje UH. Hepatitis B virus DNA levels and outcomes in chronic hepatitis B. Hepatology. 2009; 49:S72–S84. [PubMed: 19399801]

Chen CJ, Yang HI, Su J, Jen CL, You SL, Lu SN, Huang GT, Iloeje UH. Risk of hepatocellular carcinoma across a biological gradient of serum hepatitis B virus DNA level. JAMA : the journal of the American Medical Association. 2006; 295:65–73. [PubMed: 16391218]

Chen W, Jin W, Hardegen N, Lei KJ, Li L, Marinos N, McGrady G, Wahl SM. Conversion of peripheral CD4+CD25- naive T cells to CD4+CD25+ regulatory T cells by TGF-beta induction of transcription factor Foxp3. J Exp Med. 2003; 198:1875–1886. [PubMed: 14676299]

Curiel TJ, Coukos G, Zou L, Alvarez X, Cheng P, Mottram P, Evdemon-Hogan M, Conejo-Garcia JR, Zhang L, Burow M, et al. Specific recruitment of regulatory T cells in ovarian carcinoma fosters immune privilege and predicts reduced survival. Nat Med. 2004; 10:942–949. [PubMed: 15322536]

Delaney, WEt; Isom, HC. Hepatitis B virus replication in human HepG2 cells mediated by hepatitis B virus recombinant baculovirus. Hepatology. 1998; 28:1134–1146. [PubMed: 9755254]

Ding J, Huang S, Wu S, Zhao Y, Liang L, Yan M, Ge C, Yao J, Chen T, Wan D, et al. Gain of miR-151 on chromosome 8q24.3 facilitates tumour cell migration and spreading through downregulating RhoGDIA. Nat Cell Biol. 2010; 12:390–399. [PubMed: 20305651]

Ding Q, Xia W, Liu JC, Yang JY, Lee DF, Xia J, Bartholomeusz G, Li Y, Pan Y, Li Z, et al. Erk associates with and primes GSK-3beta for its inactivation resulting in upregulation of beta-catenin. Molecular cell. 2005; 19:159–170. [PubMed: 16039586]

Esquela-Kerscher A, Slack FJ. Oncomirs - microRNAs with a role in cancer. Nat Rev Cancer. 2006; 6:259–269. [PubMed: 16557279]

Feitelson MA, Duan LX. Hepatitis B virus X antigen in the pathogenesis of chronic infections and the development of hepatocellular carcinoma. Am J Pathol. 1997; 150:1141–1157. [PubMed: 9094970]

Feng YX, Wang T, Deng YZ, Yang P, Li JJ, Guan DX, Yao F, Zhu YQ, Qin Y, Wang H, et al. Sorafenib suppresses postsurgical recurrence and metastasis of hepatocellular carcinoma in an orthotopic mouse model. Hepatology. 2011; 53:483–492. [PubMed: 21274870]

Han Z. Recent progress in genomic [corrected] research of liver cancer. Science in China Series C, Life sciences / Chinese Academy of Sciences. 2009; 52:24–30.

He L, He X, Lim LP, de Stanchina E, Xuan Z, Liang Y, Xue W, Zender L, Magnus J, Ridzon D, et al. A microRNA component of the p53 tumour suppressor network. Nature. 2007; 447:1130–1134. [PubMed: 17554337]

Herceg Z, Paliwal A. Epigenetic mechanisms in hepatocellular carcinoma: how environmental factors influence the epigenome. Mutation research. 2011; 727:55–61. [PubMed: 21514401]

Jemal A, Bray F, Center MM, Ferlay J, Ward E, Forman D. Global cancer statistics. CA Cancer J Clin. 2011; 61:69–90. [PubMed: 21296855]

Kew MC. Hepatitis B virus × protein in the pathogenesis of hepatitis B virus-induced hepatocellular carcinoma. Journal of gastroenterology and hepatology. 2011; 26(Suppl 1):144–152. [PubMed: 21199526]

Lin DX, Zhang QY, Li X, Ye QW, Lin F, Li LL. An aggressive approach leads to improved survival in hepatocellular carcinoma patients with portal vein tumor thrombus. J Cancer Res Clin Oncol. 2010

Liu Y, Zhang P, Li J, Kulkarni AB, Perruche S, Chen W. A critical function for TGF-beta signaling in the development of natural CD4+CD25+Foxp3+ regulatory T cells. Nature immunology. 2008; 9:632–640. [PubMed: 18438410]

Lujambio A, Lowe SW. The microcosmos of cancer. Nature. 2012; 482:347–355. [PubMed: 22337054]

Lupberger J, Hildt E. Hepatitis B virus-induced oncogenesis. World journal of gastroenterology : WJG. 2007; 13:74–81. [PubMed: 17206756]

Mailloux AW, Young MR. Regulatory T-cell trafficking: from thymic development to tumor-induced immune suppression. Critical reviews in immunology. 2010; 30:435–447. [PubMed: 21083525]

Marotta F, Vangieri B, Cecere A, Gattoni A. The pathogenesis of hepatocellular carcinoma is multifactorial event. Novel immunological treatment in prospect. Clin Ter. 2004; 155:187–199. [PubMed: 15344567]

Massague J. TGFbeta in Cancer. Cell. 2008; 134:215–230. [PubMed: 18662538]

Matsuzaki K. Modulation of TGF-beta signaling during progression of chronic liver diseases. Frontiers in bioscience : a journal and virtual library. 2009; 14:2923–2934. [PubMed: 19273245]

Morecki S, Yacovlev L, Slavin S. Effect of indomethacin on tumorigenicity and immunity induction in a murine model of mammary carcinoma. Int J Cancer. 1998; 75:894–899. [PubMed: 9506535]

Nicoloso MS, Spizzo R, Shimizu M, Rossi S, Calin GA. MicroRNAs--the micro steering wheel of tumour metastases. Nat Rev Cancer. 2009; 9:293–302. [PubMed: 19262572]

Ouyang W, Beckett O, Ma Q, Li MO. Transforming growth factor-beta signaling curbs thymic negative selection promoting regulatory T cell development. Immunity. 2010; 32:642–653. [PubMed: 20471291]

Parkin DM, Bray F, Ferlay J, Pisani P. Global cancer statistics, 2002. CA Cancer J Clin. 2005; 55:74–108. [PubMed: 15761078]

Portolani N, Coniglio A, Ghidoni S, Giovanelli M, Benetti A, Tiberio GA, Giulini SM. Early and late recurrence after liver resection for hepatocellular carcinoma: prognostic and therapeutic implications. Ann Surg. 2006; 243:229–235. [PubMed: 16432356]

Quezada SA, Peggs KS, Curran MA, Allison JP. CTLA4 blockade and GM-CSF combination immunotherapy alters the intratumor balance of effector and regulatory T cells. The Journal of clinical investigation. 2006; 116:1935–1945. [PubMed: 16778987]

Sakaguchi S. Naturally arising CD4+ regulatory t cells for immunologic self-tolerance and negative control of immune responses. Annu Rev Immunol. 2004; 22:531–562. [PubMed: 15032588]

Schmierer B, Hill CS. TGFbeta-SMAD signal transduction: molecular specificity and functional flexibility. Nat Rev Mol Cell Biol. 2007; 8:970–982. [PubMed: 18000526]

Shevach EM. CD4+ CD25+ suppressor T cells: more questions than answers. Nature reviews Immunology. 2002; 2:389–400.

Shi J, Lai EC, Li N, Guo WX, Xue J, Lau WY, Wu MC, Cheng SQ. Surgical treatment of hepatocellular carcinoma with portal vein tumor thrombus. Ann Surg Oncol. 2010; 17:2073–2080. [PubMed: 20131013]

Siemens H, Jackstadt R, Hunten S, Kaller M, Menssen A, Gotz U, Hermeking H. miR-34 and SNAIL form a double-negative feedback loop to regulate epithelial-mesenchymal transitions. Cell Cycle. 2011; 10:4256–4271. [PubMed: 22134354]

Takizawa D, Kakizaki S, Sohara N, Sato K, Takagi H, Arai H, Katakai K, Kojima A, Matsuzaki Y, Mori M. Hepatocellular carcinoma with portal vein tumor thrombosis: clinical characteristics, prognosis, and patient survival analysis. Dig Dis Sci. 2007; 52:3290–3295. [PubMed: 17394062]

Tian J, Tang ZY, Ye SL, Liu YK, Lin ZY, Chen J, Xue Q. New human hepatocellular carcinoma (HCC) cell line with highly metastatic potential (MHCC97) and its expressions of the factors associated with metastasis. British journal of cancer. 1999; 81:814–821. [PubMed: 10555751]

Wang T, Hu HS, Feng YX, Shi J, Li N, Guo WX, Xue J, Xie D, Liu SR, Wu MC, et al. Characterisation of a novel cell line (CSQT-2) with high metastatic activity derived from portal vein tumour thrombus of hepatocellular carcinoma. British journal of cancer. 2010; 102:1618–1626. [PubMed: 20461085]

Xiong Y, Fang JH, Yun JP, Yang J, Zhang Y, Jia WH, Zhuang SM. Effects of microRNA-29 on apoptosis, tumorigenicity, and prognosis of hepatocellular carcinoma. Hepatology. 2010; 51:836–845. [PubMed: 20041405]

HIGHLIGHTS

- HBV-positive status predispose HCC patients to develop PVTT
- MiR-34a expression inversely correlates with TGFβ activity & PVTT
- HBV-induced TGFβ recruits Treg cells via suppression of miR-34a and induction of CCL22
- TGFβ-miR-34a-CCL22 promotes tumor growth and metastasis via changing microenvironment

SIGNIFICANCE

Immune-surveillance imposed by a functionally active immune system represents a critical barrier to prevent disseminated tumor cells from forming metastasis. Tumor cells need to acquire specific activities to breach this barrier to successfully colonize a new tissue microenvironment. Emerging evidence also indicates that specific pathways are activated and utilized by tumors initiated by different etiological factors. In this regard, the findings presented here support the notion that HCC initiated by HBV infection could acquire the ability to recruit immune-suppressive Treg cells via activation of the TGF-β signaling pathway, consequently promoting the formation of a particular type of intrahepatic metastasis. Meanwhile, identification of components of this pathway also provides potential therapeutic targets for the treatment of this deadly disease.

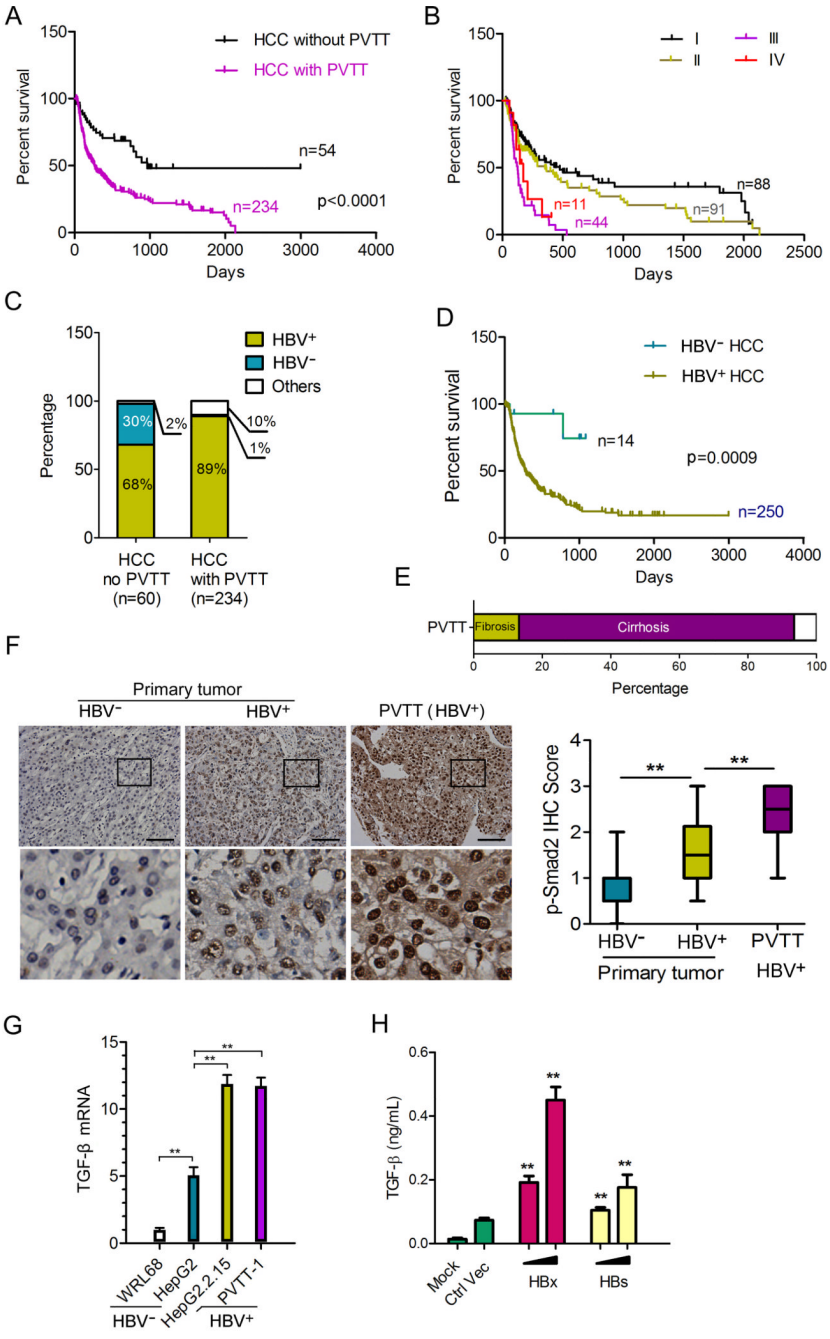

Figure 1. HBV infection status and TGF-β signaling activity are associated with development of PVTT in human HCC patients

(A) Kaplan-Meier Survival curves of HCC patients with PVTT in comparison with those without PVTT detected at the time of surgical operation. Clinical characteristics of those patients are presented in Table 1.

(B) Kaplan-Meier survival curves of HCC patients shown in Table 1 with different degree of PVTT development based on the extent of venous tumor thrombus formation. Type I: Tumor thrombi involving segmental branches of the portal vein or above; Type II: Tumor thrombi involving right/left portal vein; Type III: Tumor thrombi involving the main portal vein trunk; Type IV: Tumor thrombi involving the superior mesenteric vein.

(C) Percentage of HBV infection in HCC patients with PVTT compared with those without PVTT. “Others” in the PVTT group include 3 HCV^+ patients and 20 patients without the information of their hepatitis viral infection status. “Others” in the HCC without PVTT group include 1 HCC patient without information of hepatitis viral infection status, as well as 6 additional patients who were HBV^- that were not a part of the original set of the 288 patients analyzed in panels A and B.
(D) Kaplan-Meier survival curves of HBV^+ verses HBV^- patients with HCC. The HBV^+ group includes 41 HCC patients without PVTT and 209 HCC patients with PVTT; The HBV^- group includes 12 HCC patients without PVTT and 2 HCC patients with PVTT. 30 of the 294 patients displayed in panel C were excluded from this analysis due to the lack of specific information: 6 HBV^- patients without PVTT lack survival information; 21 patients lack hepatitis viral infection status; and 3 HCV^+ HCC patients.
(E) Rate of occurrence of pathological symptoms associated with liver cirrhosis or fibrosis in the 234 HCC patients with PVTT shown in Table 1.
(F) IHC of phosphorylated Smad2 in HCC samples. Left: Representative pictures showing different intensities of nuclear staining of pSmad2. Scale bars, 100μm. Lower panels represent magnified pictures (5X) of boxed area in the corresponding upper panels. Right: Box plot graph showing the quantitative evaluation of pSmad2 staining intensity from a tissue microarray. Plot of a box-plot (25%–75%) with whiskers to minimal and maximal of all the score data was used. The statistical differences between the three groups were analyzed by one-way analysis of variance. $^{**}p<0.01$.
(G) TGF-β expression levels in four different liver cell lines. Relative TGF-β1 mRNA level was measured by qRT-PCR and normalized to β-actin. $^{**}p<0.01$, N=3.
(H) 10^5 HepG2 cells were transfected with 0.5 μg and 1 μg HBx or HBs expression construct, respectively. 24 hrs later, relative amounts of TGF-β1 secreted into the culture media were determined by ELISA. $^{**}p<0.01$ *vs.* control vector group, N=3.
All error bars indicate mean±SD. See also Figure S1.

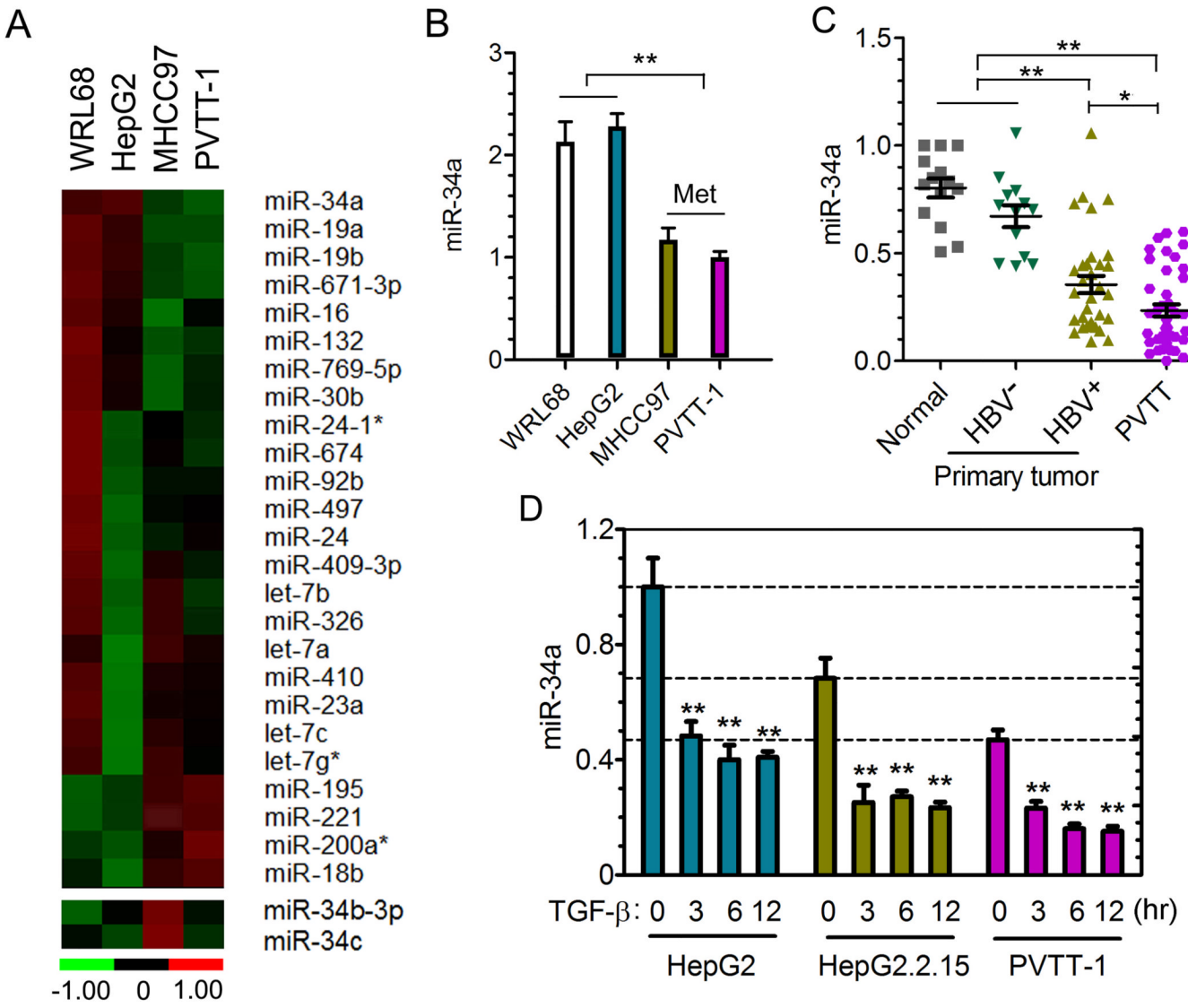

Figure 2. Reduced expression of miR-34a is correlated with HBV-positive HCC-PVTT and regulated by TGF-β

(A) Heat map of a partial list of microRNAs whose expression levels differ among the indicated four liver cell lines as determined using an RT-PCR-based miRNA expression array.

(B) The relative level of miR-34a of indicated cell lines was measured by qRT-PCR and normalized to the level of U6. N=3. **p<0.01 calculated by student's t test.

(C) The relative level of miR-34a in 26 PVTT tissue samples (all HBV^+), 30 primary tumor tissue samples (17 HBV^+ and 13 HBV^-), and 14 normal liver tissues distal to tumor regions was determined by qRT-PCR and normalized to U6. **p<0.01 calculated by student's t test.

(D) The relative level of miR-34a in different cell lines mock-treated or treated with TGF-β1 for indicated time points was measured by qRT-PCR and normalized to U6. N=3. **p<0.01 calculated by student's t test.

All error bars indicate mean±SD. See also Table S1, Figure S2.

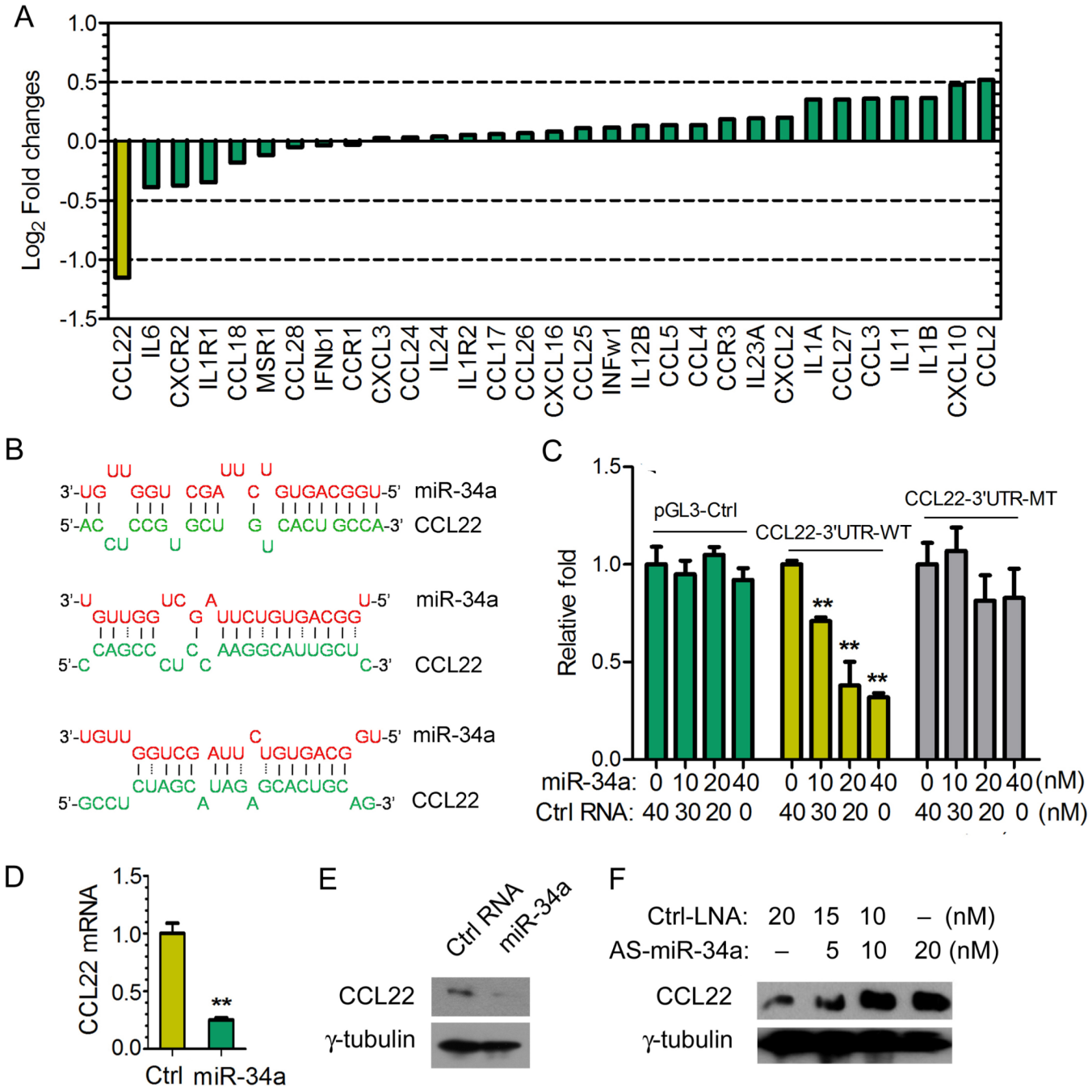

Figure 3. The chemokine CCL22 is a *bona fide* target of miR-34a

(A) PVTT-1 cells were transfected with 80 nM of pre-miR-34a mimetic oligos and a RT-PCR-based expression array was carried out to determine the expression profile of 94 cytokines, chemokines and their receptors 6 hrs later. The expression pattern for 31 out of the 94 genes is presented as representatives.

(B) Putative miR-34a binding sites in the 3'-UTR of human *CCL22*.

(C) HEK293T cells were transiently transfected with pre-miR-34a mimetic or control oligos together with the pGL3 control plasmid, a modified pGL3 plasmid containing the wild type CCL22 3'UTR or a mutant CCL22 3'UTR with all three putative target sequences mutated. Pre-miR-34a mimetic or control oligos were added at the indicated concentrations and the

luciferase activity was analyzed 24 hrs later. Data is presented as relative firefly luciferase units normalized with the value of renilla luciferase. N=3. ** p<0.01 (Student t-test).
(D) PVTT-1 cells were transfected with 80 nM of pre-miR-34a mimetic oligos and the CCL22 mRNA level was determined by qPCR 48 hrs later and normalized to GAPDH. **p<0.01 (Student t-test).
(E) PVTT-1 cells were treated as in panel D and CCL22 protein level in culture media was determined by Western blot. γ-tubulin in corresponding cell lysates was used as a loading control. N=3.
(F) PVTT-1 cells were transfected with AS-miR-34a or control oligos at the indicated concentrations and the CCL22 level in culture media was determined by Western blot 48 hrs later. γ-tubulin in corresponding cell lysates was used as a loading control. N=3.
All error bars indicate mean±SD. See also Figure S3.

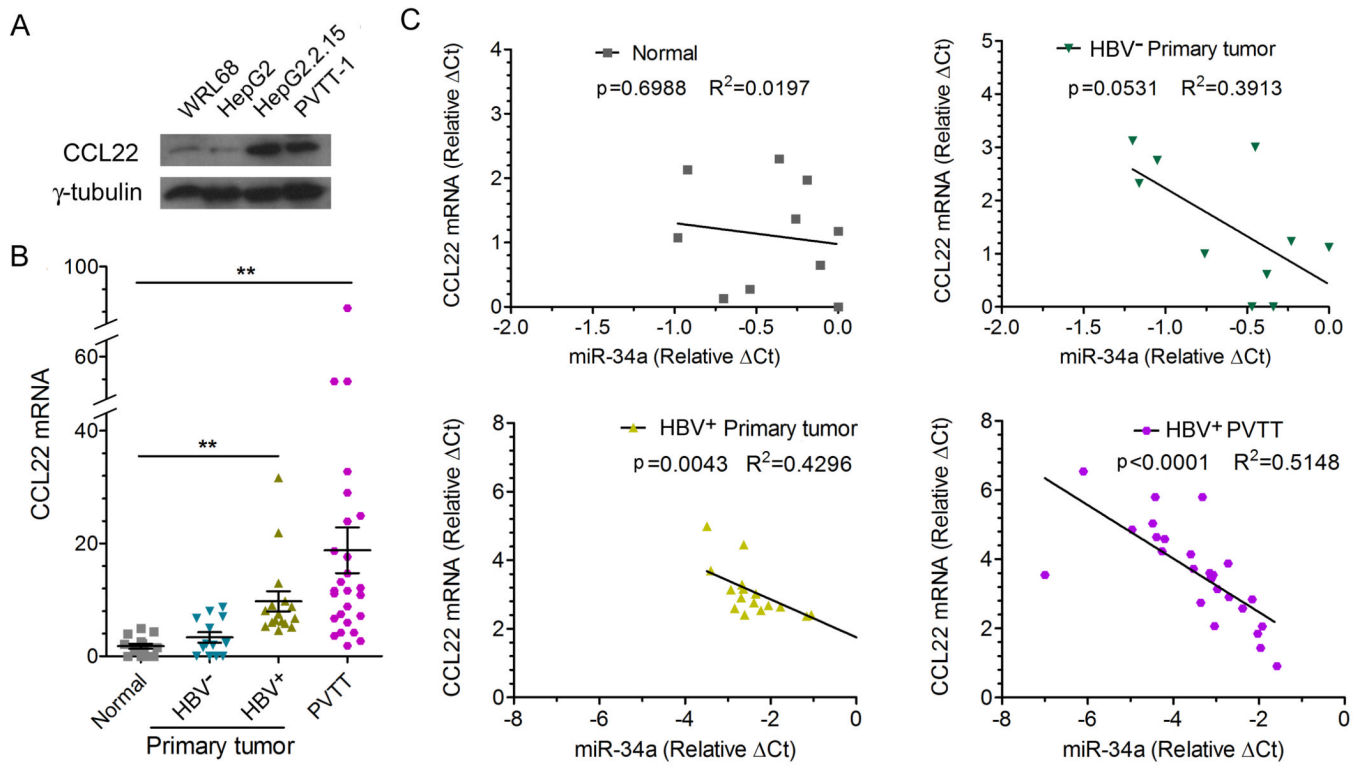

Figure 4. CCL22 up-regulation in PVTT is associated with down-regulation of miR-34a

(A) The CCL22 protein level in indicated liver cell lines was determined by Western blot. γ-tubulin was used as a loading control.

(B) Tissue specimens from the same set of patients as in Figure 2C were examined for the mRNA level of CCL22 by qRT-PCR and normalized to that of β-actin (CCL22 mRNA was undetectable in 4 normal liver tissues and 2 HBV^- HCC primary tumor tissues). *p<0.05, **p<0.01 (Student t-test). Mean±SD.

(C) Clinical samples from the same set of specimen as in Figures 2C and 4B were analyzed in the four groups as indicated (CCL22 mRNA was undetectable in 4 normal liver tissues and 2 HBV^- HCC primary tumor tissues). The correlation between miR-34a and CCL22 expression for each individual was assessed by linear regression.

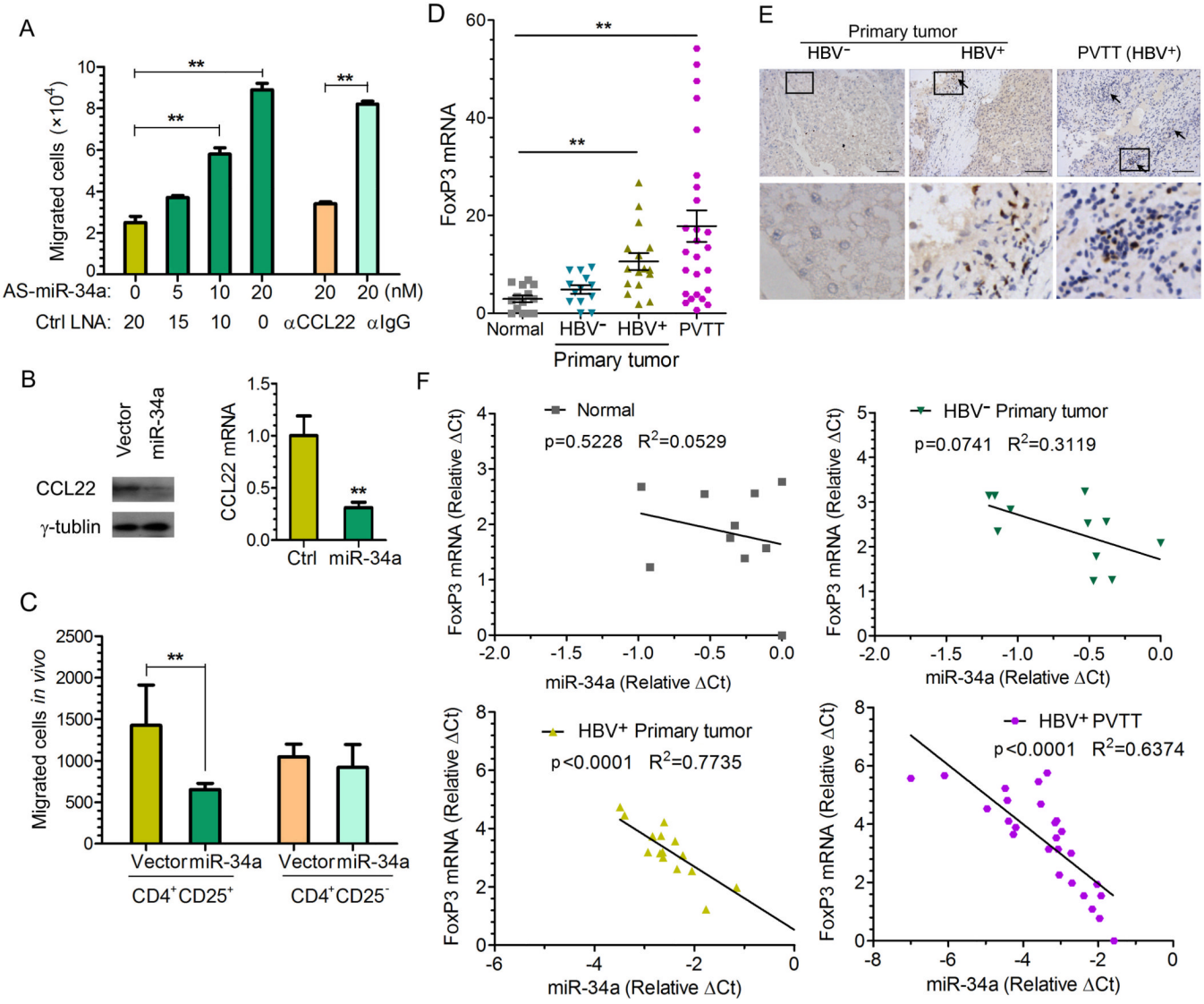

Figure 5. The miR-34a-CCL22 pathway regulates CD4$^+$CD25$^+$ Treg cell recruitment into the tumor microenvironment

(A) 1×10^5 human CD4$^+$CD25$^+$ Treg cells were tested by transwell assay for their migration towards culture media of PVTT-1 cells harvested 24 hrs after the cells were transfected with different amounts of AS-miR-34a or control oligos as indicated. CCL22 neutralizing or control antibody was added to the culture media of AS-miR-34a oligos transfected PVTT-1 cells to determine the effect on Treg cell migration. 4 hrs after plating of the T cells in the upper chamber, migrated Treg cells were quantified by Cell Counter analysis (N=3, mean ±s.d.). **p<0.01 (Student t-test).

(B) CCL22 protein (left panel) or mRNA (right panel) level in xenograft tumors tissue samples derived from indicated PVTT-1 cells in nude mice was determined. γ-tubulin was used as a loading control for the Western blot, and mRNA level of CCL22 was normalized to that of GAPDH. N=4.

(C) Freshly isolated human CD4$^+$CD25$^+$ or CD4$^+$CD25$^-$ T cells were injected via the tail vein into nude mice with xenograft tumors formed by PVTT-1 cells ectopically expressing the vector control or miR-34a as indicated and tumors were extracted 48 hrs later. FACS

was used to quantify the number of T cells within 1×10^8 total cells from each tumor. N=4, Mean±s.d. **p<0.01 (Student t-test).

(D) The mRNA level of FoxP3 in HBV^+ HCC primary and PVTT samples from the same set of patients as in Figures 2C and 4B was measured by qRT-PCR and normalized to that of β-actin (FoxP3 mRNA was undetectable in 4 normal liver tissues and 2 HBV^- HCC primary tumor tissues). *p<0.05, **p<0.01 (Student t-test).

(E) Treg cell accumulation in HCC primary and PVTT samples was determined by immunohistochemistry staining using an anti-FoxP3 antibody. Representative pictures from one set of the samples are shown. Arrows indicate $FoxP3^+$ Treg cells stained in dark brown color. Scale bars, 100μm. Lower panel represents magnified views (5X) indicated by boxes in the upper panel.

(F) Clinical samples from the same set of patients as in Figures 2C and 5D were analyzed in four groups as indicated (FoxP3 mRNA was undetectable in 4 normal liver tissues and 2 HBV^- HCC primary tumor tissues). The correlation between miR-34a and FoxP3 expression for each individual was assessed by linear regression.

All error bars indicate mean±SD. See also Figure S4.

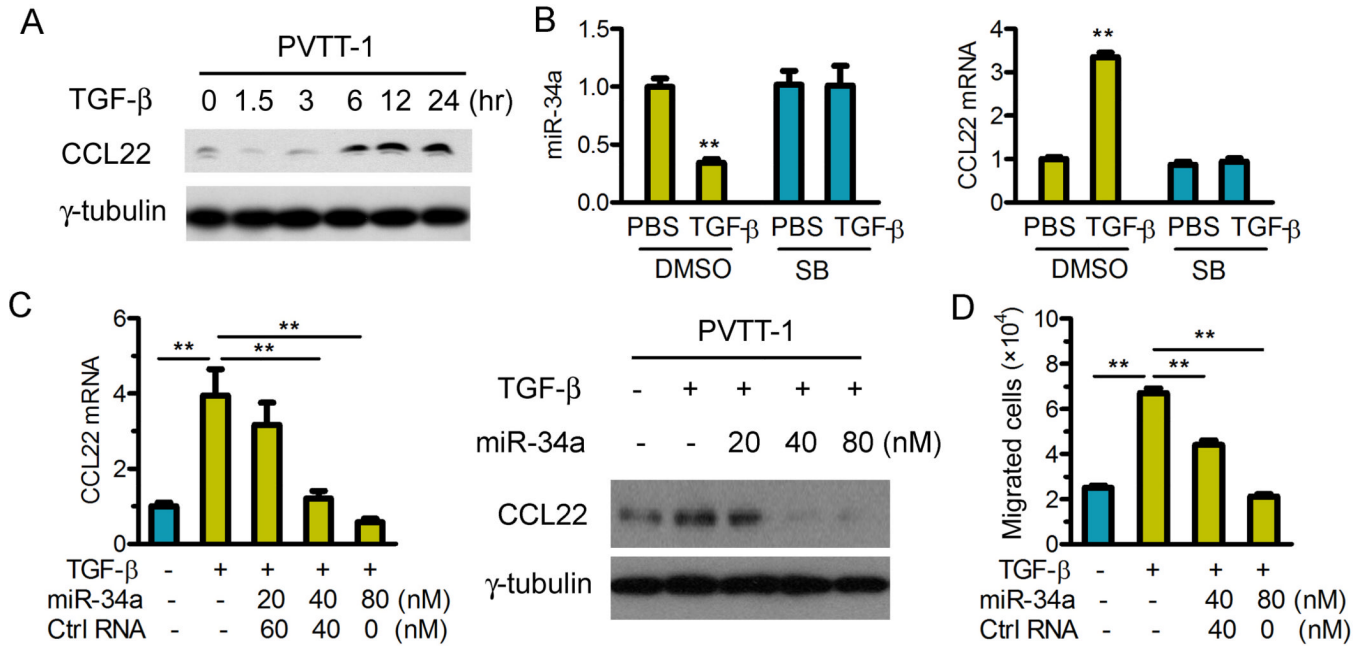

Figure 6. TGF-β positively regulates the production of CCL22 and Treg cell migration via repression of miR-34a in PVTT-1 cells

(A) Time course of TGF-β-induced CCL22 production detected in the culture media of PVTT-1 cells. CCL22 was detected by Western blot and γ-tubulin in corresponding cell lysate was used as a loading control.

(B) PVTT-1 cells were pretreated with the control solvent (DMSO) or SB431542 (SB) at 20 μM for 30 min and then treated with TGF-β1 for 12 hrs. The expression of miR-34a (left panel) and of CCL22 mRNA (right panel) were measured by qRT-PCR and normalized to U6 or GAPDH, respectively (N=3, Mean±s.d.). **p<0.01 (Student t-test).

(C) PVTT-1 cells were pretreated with various doses of pre-miR-34a mimetic or control oligos for 24 hrs, before TGF-β1 treatment for another 12 hrs as indicated. The level of CCL22 mRNA was measured by qRT-PCR and normalized to GAPDH (left panel). CCL22 protein was detected by Western blot and γ-tubulin was used as a loading control (right panel).

(D) The same transwell assay as in Figure 5A was conducted with supernatants from PVTT-1 cells first transfected with pre-miR-34a or control oligos, and 24 hrs later treated with TGF-β1 for another 24 hrs. (N=3, mean±s.d.). **p<0.01 (Student t-test).

All error bars indicate mean±SD.

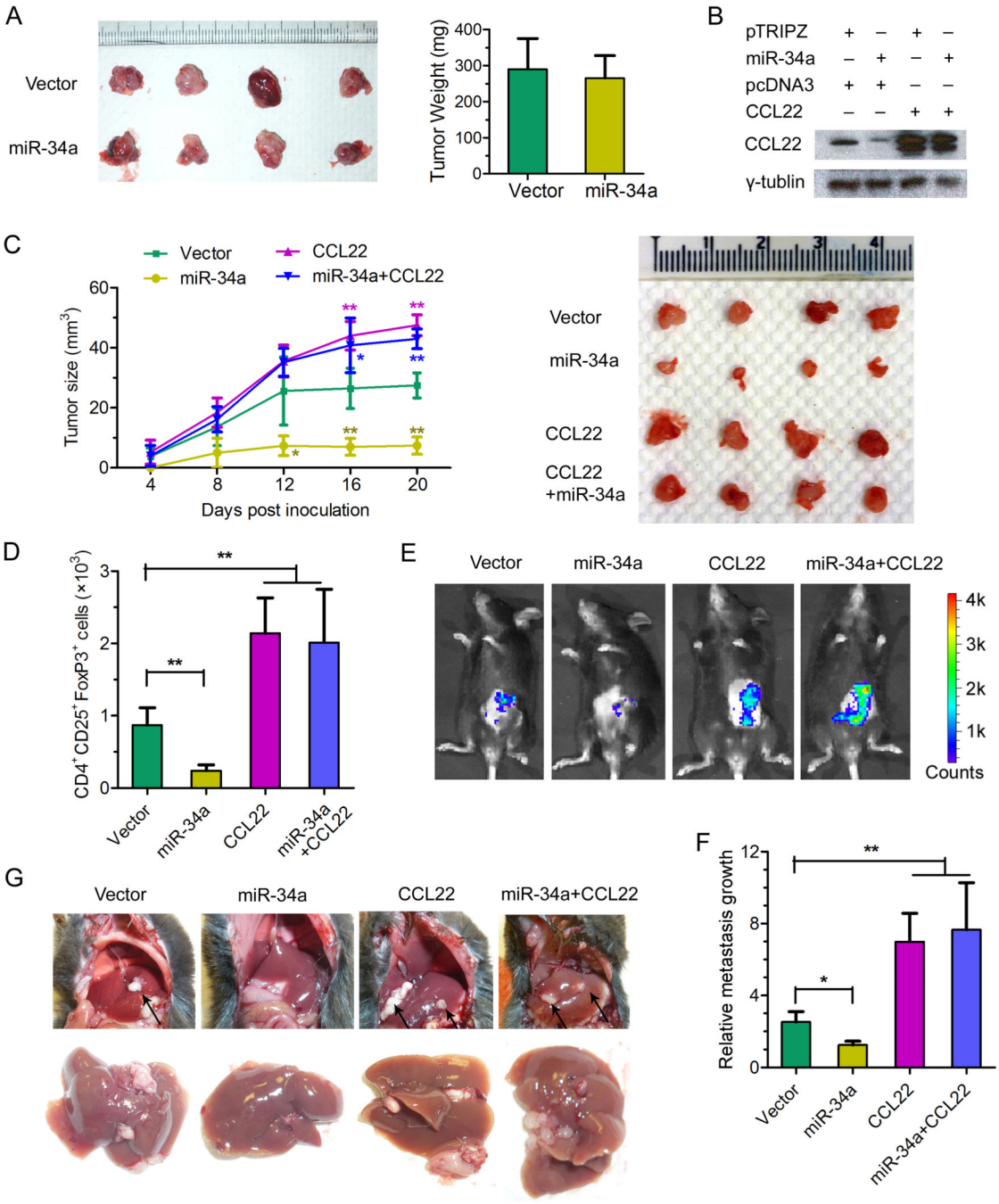

Figure 7. Impact of miR-34a and CCL22 on tumor growth and metastasis associated with Treg cell recruitment to the tumor microenvironment

(A) 5×10^5 pTRIPZ-miR-34a or pTRIPZ-mock stably transfected Hepa1-6 cells were subcutaneously injected into 6-week-old nude mice. Three weeks later, tumors derived from indicated cells were isolated and shown in the left panel with the plot of their weight displayed in the right panel. N=4.

(B) pTRIPZ-miR-34a or pTRIPZ-mock together with pcDNA3-CCL22-ORF or pcDNA3 vector as indicated were stably transfected into Hepa1-6 cells to generate population of cells. 2×10^6 of each population of those cells were subcutaneously injected into 6-week-old male C57BL/6J mice. The animals were administered Doxcycline 2μg/mouse by gavage every 2

days. After 21 days, CCL22 in tumor tissues was detected by Western blot and γ-tubulin was used as a loading control.

(C) The tumor growth curves (left panel) for the same four populations of stably transfected Hepa1-6 cells as described in panel B were measured and the tumors isolated 21 days after inoculation are pictured in the right panel. **p<0.01 (Student t-test). N=4 per experimental group; experiment repeated 3 times.

(D) Treg cells were quantified in tumors grown from the four populations of Hepa1-6 cells in C57BL/6J mice. The number of Treg cells from 50 mg of tumor tissue derived from indicated cells was determined via cell counting by flow cytometry.

(E) The same four Hepa1-6 populations as described in panel B co-expressing a luciferase reporter were introduced into the C57BL/6J mice via intrasplenic injection. After 21 days, luciferase signals derived from abdominal metastatic tumor growth as shown in the representative images were determined by the Xenogen IVIS Lumina system.

(F) Luciferase signal levels from the four groups of mice shown in panel E was normalized to that of control mice without tumor growth, and computed as the values for relative metastatic growth by each of the indicated Hepa1-6 cell populations. *p<0.05, **p<0.01 (Student t-test). N=4 per experimental group; experiment repeated 3 times.

(G) Representative pictures showing the formation of tumor metastases in the mouse liver by each of the indicated Hepa1-6 populations. Arrows indicate metastatic tumors in the mouse liver.

All error bars indicate mean±SD. See also Figure S5.

Table 1

Clinical characteristics of HCC patients with or without PVTT.

Clinical characteristics		HCC without PVTT (n=54)	HCC with PVTT (n=234)
Age	Mean±S.D.	55.89±10.25	48.08±9.43
Gender	Male/Female	43/11	211/23
Hepatitis virus	$HBsAg^+$	41	209
	$HBsAg^-$	12	2
	$HCVAb^+$	0	3
	$HBsAg^+$ $HCVAb^+$	0	0
	Unknown	1	20
Tumor number	1	46	214
	≥2	8	20
Median survival	Days	964	263
AFP (ng/mL)	<20	27	37
	≥20	27	197
Distant metastasis *	Met/Total cases	3/54	66/234

Notes: Tumor number indicates number of primary tumor mass detected at the time of surgical operation. AFP: α-fetal protein in the serum.

* Distant metastasis includes metastases to lung, bone, brain, abdominal lymph nodes, adrenal gland, and abdominal wall.